Organic Process Research & Development **2004**, *8*, 576−582

Drying an Organic Monohydrate: Crystal Form Instabilities and a Factory-Scale Drying Scheme to Ensure Monohydrate Preservation

Stephen H. Cypes,*,† Robert M. Wenslow,‡ Scott M. Thomas,‡ Alex M. Chen,‡ Jason G. Dorwart,‡ John R. Corte,‡ and Mahmoud Kaba‡

Symyx Technologies, Inc., 3100 Central Expressway, Santa Clara, California 95051, U.S.A., and Merck Research Laboratories, P.O. Box 2000, RY814-S200, Rahway, New Jersey 07065, U.S.A.

Abstract:

This contribution discusses the laboratory results and factory-scale drying of an organic monohydrate with therapeutic qualities. The crystal form instabilities of this monohydrate are discussed with respect to undesired dehydrated crystalline species and an IPA solvate. To reproducibly determine the end-of-drying while ensuring deliverable monohydrate is produced, a factory-scale drying scheme in which a dew-point hygrometer is used to measure the water content of the dryer vapor effluent online was shown to be effective. This online measurement technique obviates the need for repeated sampling from the dryer and is a low-cost alternative to near-infrared (NIR) spectroscopy monitoring systems. This novel factory-scale drying scheme was successful in determining the end-of-drying while ensuring preservation of the desired monohydrate for four 20−30 kg batches. Also, drying curves were produced from the recorded dew-point data by an iterative approach.

Introduction

When designing factory-scale drying processes of organic compounds, specifically in the pharmaceutical industry, many factors need to be considered that may ultimately affect the physical design of the dryer as well as the operating conditions. For an active pharmaceutical ingredient (API), chemical stability, crystal form (or polymorph) stability, agglomeration, granulation, and undesired particle attrition all play a role in the final design of the drying process. It is this multitude of variables that have led to more than 200 distinct dryer variations from at least 150 different manufacturers.[1]

Designing a factory-scale drying process for an API that can exist in a number of different crystal forms adds to the overall design challenge. Since the total time needed to dry a batch of wet solids (or wetcake) is dependent on wetcake properties that vary from batch to batch, simply setting a drying time specification may not be suitable for a compound that can "overdry." More specifically, crystalline hydrates may have the potential to lose crystal-bound water once residual free solvent on the wetcake has been removed, and bound water from the crystal lattice is subsequently removed by continued drying. The loss of bound water in a hydrate can have multiple effects on the final dry solids, including the appearance of amorphous material, new crystalline anhydrous species, or crystalline lower-numbered hydrates.[2−3]

Several previous solutions to determine the endpoint to drying have been presented for hydrated species.[4−7] These methods all employed the use of near-infrared (NIR) spectroscopy to quantify water content in a number of different drying schemes. NIR can either be used to quantitatively differentiate between free and bound water directly in the solids by having the NIR probe in direct contact with the wetcake[4] or be used to measure water and solvent vapor composition in the dryer effluent.[5−7] The use of NIR in either case requires extensive calibration models produced by partial least-squares regression, and it tends to be imprecise and inaccurate when measuring trace water content in the vapor phase (if water is the last solvent to be removed from the wetcake).

This contribution discusses issues related to the factory-scale drying process of an organic monohydrate (3.46 wt % water, dry basis) obtained via crystallization from 80/20 (w/w) isopropyl alcohol/water. This compound can exist in multiple undesired crystal forms, including an isopropyl alcohol (IPA) solvate and several anhydrous crystalline forms obtained by overdrying. Issues concerning the final IPA/water wash composition and the drying temperature and drying endpoint are discussed. A new factory-scale online method to determine the end-of-drying is shown to be effective for the preservation of the monohydrate during drying. The method employs a dew-point hygrometer to measure the water vapor content in the dryer effluent. The use of a similar setup has previously been shown to be effective at laboratory scale.[8]

Experimental Section

Drying Setup for the Monohydrate. Approximately 110 kg of Merck drug substance M1 (monohydrate, 3.46 wt % water, dry basis) was crystallized according to a predetermined process from isopropyl alcohol (IPA) (Shell) and DI

* To whom correspondence should be addressed. E-Mail: scypes@symyx.com.
† Symyx Technologies, Inc.
‡ Merck Research Laboratories.

(1) Cook, E. *Chem. Process.* **1999**, *62*, 36−39.
(2) Giron, D.; Goldbronn, Ch.; Mutz, M.; Pfeffer, S.; Piechon, Ph.; Schwab, Ph. *J. Therm. Anal. Calorim.* **2002**, *68*, 453−465.
(3) Laurent, S. Couture, F.; Roques, M. *Chem. Eng. Process.* **1999**, *38*, 157−165.
(4) Zhou, G.; Ge, Z.; Dorwart, J.; Izzo, B.; Kukura, J.; Bicker, G.; Wyvratt, J. *J. Pharm. Sci.* **2003**, *92*, 1058−1065.
(5) Harris, S.; Walker, D. *J. Pharm. Sci.* **2000**, *89*, 1180−1186.
(6) White, J. *Pharm. Res.* **1994**, *11*, 728−732.
(7) Coffey, C.; Predoehl, A.; Walker, D. *Appl. Spectrosc.* **1998**, *52*, 717−724.
(8) Groenewold, C.; Moser, C.; Groenewold, H.; Tsotsas, E. *Chem. Eng. J.* **2002**, *86*, 217−222.

Published on Web 05/11/2004
10.1021/op049956a CCC: $27.50

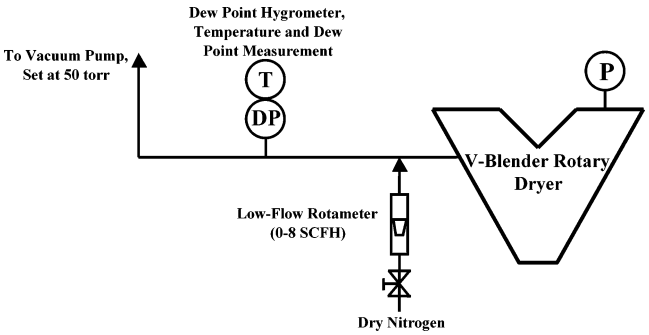

Figure 1. **Factory-scale drying setup for online monitoring of the rotary dryer vapor effluent to call the end-of-drying for the monohydrate.**

water. The wetcake was isolated using a centrifuge in four separate drops of 20−30 kg monohydrate per drop. These four separate wetcake isolations, all originating from the same crystallization batch, are named Batch 1A, Batch 1B, Batch 1C, and Batch 1D.

Each batch of wetcake was dried separately, using a V-Blender rotary dryer (Manufacturer: Paul O. Abbe Inc., 8.3 ft^3 total capacity, 5.0 ft^3 working capacity), as shown in Figure 1. The dew-point hygrometer used to monitor the dryer effluent was a Vaisala HMP260 series probe. This probe uses a thin polymer membrane that absorbs water dependent on the partial pressure of water in the surrounding vapor space and subsequently will have a change in capacitance due to the absorbed water. The polymer membrane is unaffected by the presence of IPA vapor (as well as many other common organic solvents). Dry nitrogen dilution in the dryer effluent was installed to prevent possible condensation on the dew-point probe, although this was never needed during the experiments. All batches were dried with 40 °C water on the dryer jacket and 45−60 Torr absolute pressure.

Thermogravimetric Analysis (TGA). Isothermal dehydration curves were produced using a Perkin-Elmer TGA 7 or Pyris 1 thermogravimetric analyzer. Continuous dry nitrogen (RH < 0.8% at 25 °C, dew point = −37 °C) flow was maintained over the sample at 40 mL/min.

Dynamic Vapor Sorption Analysis (DVS). Vapor sorption isotherms were produced using Symmetric vapor sorption analyzer (SGA-100) by VTI Corporation at various temperatures with humidity controlled by mixing dry nitrogen (RH < 0.8% at 25 °C, dew point = −37 °C) with humid nitrogen produced by saturating dry nitrogen with a water bath. The dew point of the humidified nitrogen stream was measured with a chilled mirror dew-point analyzer, and the relative humidity in the chamber was calculated using the standard DVS balance software. The flow rate of humid nitrogen over the previously dried monohydrate was 175 sccm.

X-ray Diffraction Analysis (XRD). XRPD analysis was used to confirm crystalline form. The diffraction pattern was generated on a Philips Analytical X'Pert PRO X-ray diffraction system with PW3040/60 console. A PW3373/00 ceramic Cu LEF X-ray tube Kα radiation was used as the source. All XRPD patterns were compared to standards for the known polymorphs of drug substance M1.

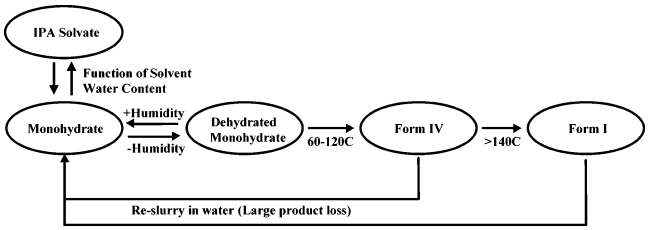

Figure 2. **Polymorphic relationships for the desired monohydrate.**

Karl Fischer Titration Analysis (KF). Water determination was performed by Karl Fischer titration analysis. Using a Metrohm 701 KF titrator (Brinkmann), 250−350 mg of the monohydrate was weighed and titrated to the endpoint using pretitrated methanol as the vessel solution.

Gas Chromatography Analysis (GC). 2-Propanol determination was performed by gas chromatography (GC), using a Hewlett-Packard (HP) 5890 GC system equipped with a HP-7673 injector. The GC column used was an RTX-1701, 30 m × 0.32 mm i.d. with a 1.0 μm film thickness. The flow rate was accomplished by setting the column head pressure at 10 psi. Injections of 1.0 μL were made into a split/splitless injector equipped with a deactivated glass liner at 200 °C. The spilt ratio for the sample injections was 20:1. Detection was performed using a flame ionization detector at 240 °C. The hydrogen flow to the detector was 300 mL/min, and the air flow was 30 mL/min. IPA solutions were prepared at concentrations of 0.01, 0.005, and 0.001% v/v in distilled water. Sample solutions were prepared at 50 mg/mL, also in distilled water. The weight percent IPA was calculated as follows:

$$\text{wt \% IPA} = \frac{(A_x - A_b) \times (C_s) \times (\rho)}{(A_s - A_b) \times (W)}$$

A_x = peak area in the sample

A_b = peak area in the blank

A_s = average peak area in the standard

C_s = concentration of the standard in volume %

ρ = density of solvent (g/mL)

W = sample concentration (g/mL)

Results

Polymorphic Relationships and Preservation of the Monohydrate. Predetermined polymorphic relationships for the monohydrate of drug substance M1 are shown in Figure 2. (The determination of the thermodynamic boundaries of this relationship is being detailed in a future manuscript.) This figure shows two possible crystal form instabilities for the monohydrate that can occur during the drying process: (1) During drying, the IPA/water residual solvent ratio on the wetcake could be such that the IPA solvate is the more favorable polymorph, and (2) overdrying the monohydrate can result in the formation of dehydrated monohydrate and Form IV or Form I anhydrous crystalline forms.

To ensure that the IPA solvate will never be favored during drying, a water activity plot for the IPA solvate and

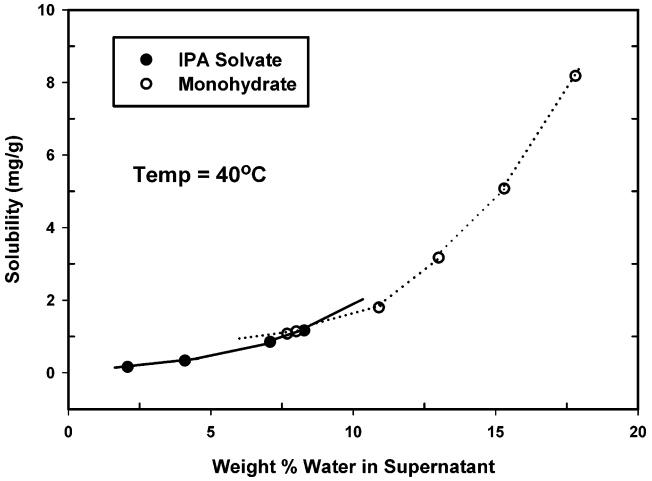

Figure 3. **Water activity plot showing relative stability of the monohydrate and IPA solvate at 40 °C.**

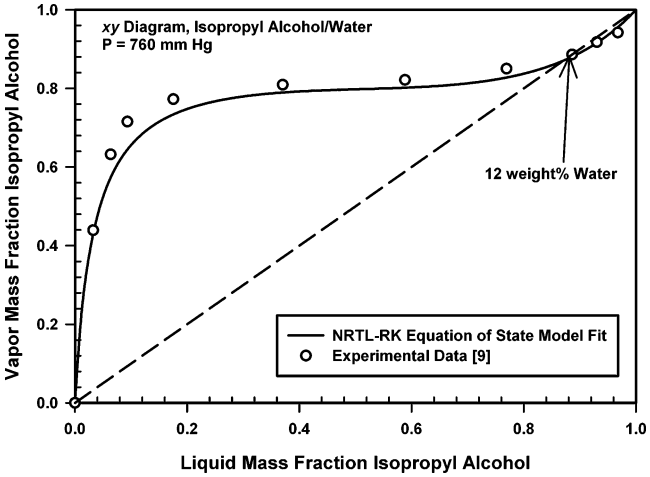

Figure 4. ***xy*-diagram for IPA/water comparing simulation and published results. There is an azeotrope in this system at 12 wt % water.**

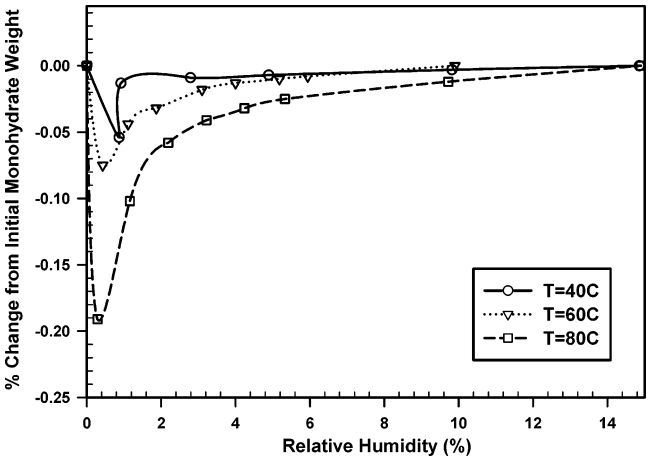

Figure 5. **Vapor sorption isotherms at T = 40, 60, 80 °C showing water loss from the monohydrate as a function of humidity and temperature.**

monohydrate was produced in IPA/water at 40 °C. This plot is shown as Figure 3, in which the solubilities of each polymorph are given as a function of IPA/water compositions. Since solubility is directly related to Gibbs free energy, the polymorph with the lower solubility at any given condition will be the more favored crystal form. As can be seen in Figure 3, the IPA solvate is favored when the water content is less than ∼8 wt % in the supernatant and the monohydrate is favored above ∼8 wt % water in the supernatant at 40 °C.

To ensure that the solvent composition on the wetcake remained >8 wt % water during the course of drying, it was desirable to preferentially remove the IPA from the wetcake at a rate faster than that for the water. This can be achieved by choosing a final wetcake wash composition in which the IPA is more volatile than the water. Simply washing with pure water (our solvent) is not an option since drug substance M1 has >100 mg/g solubility in water, whereas washing with pure IPA (our antisolvent) is not an option since the undesired IPA solvate will become the favored polymorph.

Vapor−liquid equilibrium (VLE) data for IPA/water was obtained by simulation using ASPEN Simulation Software (version 11.1.1) and the NRTL-RK Equation of State. Figure 4 shows this simulation result as an *xy*-diagram, along with previously published data for this system.[9] As can be seen in the plot, the simulation accurately predicts an azeotrope at ∼12 wt % water. Also, it has been shown that the azeotropic composition changes negligibly with pressure, and therefore the azeotropic estimate of 12 wt % water is valid under vacuum conditions.[9]

Using both the water activity plot shown in Figure 3, as well as the *xy*-diagram shown in Figure 4, a final wetcake wash composition of 80/20 (w/w) IPA/water ensures that IPA will be more volatile than water when drying and will, therefore, be preferentially removed. This results in a solvent composition on the wetcake that is always greater than 8 wt % water, and therefore the desired monohydrate is the favored polymorph during the entire course of drying.

A second instability for the monohydrate during drying can occur if the monohydrate is overdried, resulting in the formation of dehydrated monohydrate, anhydrous crystalline Form IV, and/or anhydrous crystalline Form I (see Figure 2). Therefore, the dynamics of dehydrated monohydrate formation were studied to determine how to avoid forming the dehydrated species during drying.

Dynamic vapor sorption (DVS) isotherms were obtained to determine the minimum relative humidity (RH) needed to preserve the monohydrate as a function of temperature. The results are shown in Figure 5. As can be seen in this plot, the monohydrate does not lose any appreciable weight when the RH is greater than ∼0.8% at 40 °C, greater than ∼4% at 60 °C, and greater than ∼6% at 80 °C. This DVS data suggest that a humid nitrogen sweep to the dryer would be sufficient to preserve the monohydrate by eliminating the possibility of dehydration.

To understand the kinetics of dehydration under a dry nitrogen sweep, isothermal TGA experiments were performed to profile the crystalline water weight loss as a function of time at various temperatures. These profiles are shown in Figure 6 for temperatures ranging from 40 to 90 °C. As can be seen, the monohydrate lost all 3.46 wt % of

(9) *International Critical Tables of Numerical Data, Physics, Chemistry and Technology*, 1st electronic ed.; Knovel: New York, 2003; Vol. III, p 310.

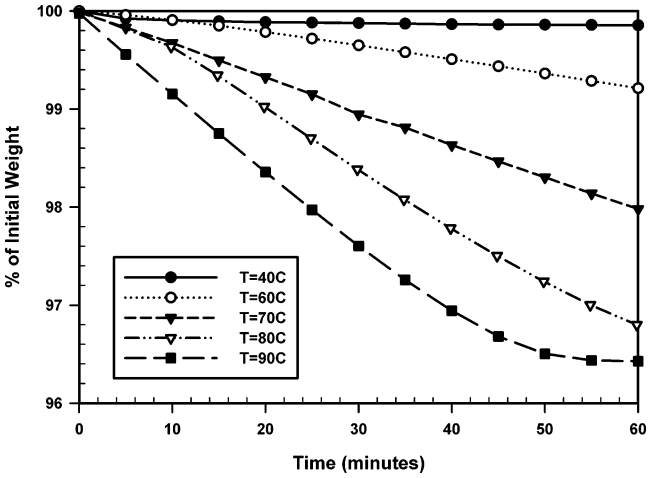

Figure 6. **Isothermal TGA dehydration curves showing temperature dependence of monohydrate dehydration.**

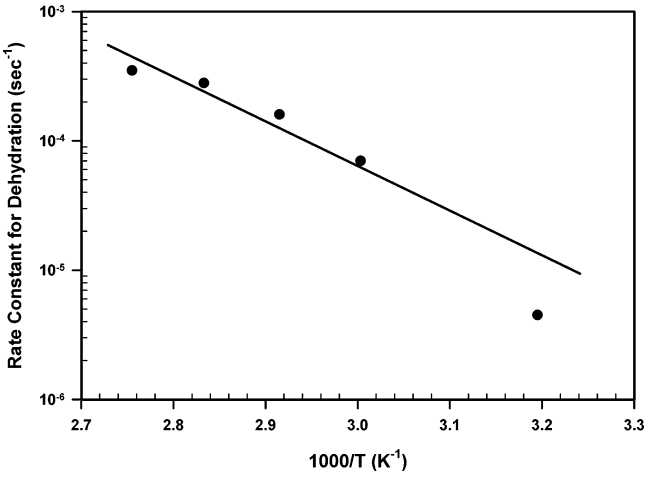

Figure 7. **Arrhenius dependence on the rate of dehydration as a function of temperature.**

its crystalline water in less than 1 h at 90 °C. Also, the rate of dehydration is linear (i.e., zero-order) and decreases substantially as the temperature decreases.

The TGA data suggest a specific mechanism of dehydration under the experimental conditions. As suggested in previous literature,[10] dehydration occurs as a three-step process: (1) bound water overcomes an activation energy barrier to become mobile water in the crystal lattice, (2) the water molecule diffuses to the crystal surface, and (3) the water is removed into the carrier gas via a convective mass-transfer process.

The data presented in Figure 6 suggest that the rate-limiting step for dehydration from 40 to 90 °C is not diffusion of the water molecule to the crystal surface. If this were the case, the dehydration profile would not be linear since water molecules further from the surface would take longer to be removed from the crystal, resulting in a decrease in the dehydration rate over time. The data also suggest that the rate-limiting step for this temperature range is not mass transfer to the carrier gas, since mass transfer is mainly flow-rate dependent and only a weak function of temperature. If the dehydration were mass-transfer dependent, there would be no appreciable difference in the dehydration rate as a function of temperature. Therefore, it can be assumed that the rate-limiting step for water removal from the monohydrate is the rate in which bound water in the crystal lattice becomes mobile.

Plotting the rate constant for dehydration, calculated as the negative slope of the dehydration profile, as a function of temperature, shows an Arrhenius dependence as seen in Figure 7. This is consistent with the conclusion presented earlier in which the rate of dehydration is limited by the activation energy barrier for crystal-bound water to become mobile water. The apparent activation energy for this mechanism can be calculated by determining the slope of the line in Figure 7, which is equal to $-E_A/R$. By this method, E_A is calculated to be 46.2 ± 8.2 kJ/mol.

Due to the high effective sweep rate in the TGA experiments, the data represent the fastest that dehydration can occur at various temperatures. At factory-scale, dehydration will occur at a rate similar to that as given by the TGA data given for a similar particle size (such that water diffusion does not become rate limiting) and given a sweep rate comparable to that of the TGA experiments. However, the rate of dehydration at factory-scale may be less than the TGA data if the sweep rate is slow enough such that mass transfer of water to the carrier gas becomes the rate-limiting step.

Factory-Scale Drying Process for Preservation of the Monohydrate. To use existing factory equipment with minimal modifications, it was desirable to design a drying protocol for the monohydrate in an existing rotary dryer. It is typically very difficult to introduce a sweep, such as humid nitrogen, into a rotary dryer without extensive mechanical enhancements. Therefore, using humidity to preserve the monohydrate during drying was not preferable. As a result, a drying process was designed to reduce the risk of dehydration in the absence of a sweep.

The TGA data presented in Figure 6 showed a temperature dependence on the rate of dehydration with an effective dry nitrogen sweep of ~2000 mL·g^{-1}·min^{-1}. This sweep rate was calculated by taking the dry nitrogen flow rate during the TGA experiments of 40 mL/min and dividing by the total dry monohydrate sample size to obtain the dry nitrogen sweep rate per weight of solids. As can be seen in Figure 6, a temperature of 40 °C resulted in a fairly slow dehydration (62 h for complete loss of crystalline water) yet would still supply enough heat in the factory process to dry the wetcake with a reasonable time cycle.

To test the stability of the monohydrate in a factory-scale rotary dryer, 5 kg of nearly dry monohydrate was charged to the dryer. A vacuum test on the dryer resulted in a calculated leak rate of ~1.7 mol/min at $P = 50$ mmHg. This leak rate acts like an effective sweep during drying in vacuo. The jacket temperature on the dryer was set to 40 °C, and constant rotation at 3 rpm and vacuum at 45−60 mmHg were maintained during the experiment. To calculate the humidity in the dryer, the ambient dew point was measured at ambient conditions with the dew-point hygrometer. By using dew-

(10) Konishi, Y.; Kobayashi, M. *J. Food Eng.* **2003**, *59*, 277−283.

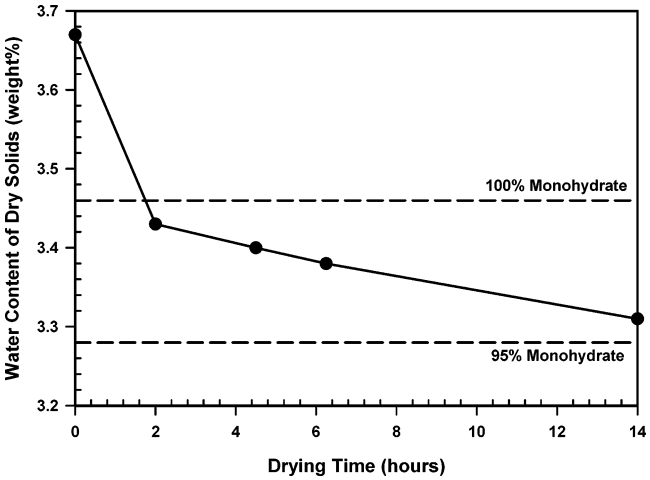

Figure 8. **Dehydration profile for a 5-kg batch of monohydrate in the factory-scale rotary dryer as the batch is "overdried."**

point/frost-point tables,[11−12] this measured dew point was converted to a partial pressure of water. The relative humidity in the dryer can then be calculated using eq 1 and was determined to be 0.4% by this method. On the basis of the DVS data presented in Figure 5, this humidity was determined to be low enough in the dryer such that the monohydrate will not be indefinitely preserved at 40 °C.

$$\mathrm{RH}_{\mathrm{dryer}} = \frac{P^{\mathrm{atm}}_{\mathrm{H_2O}} \times P_{\mathrm{dryer}}}{P^{\mathrm{sat}}_{T=40\mathrm{C}} \times P_{\mathrm{atm}}} \times 100\% \qquad (1)$$

Samples were pulled from the dryer every several hours to profile the rate of dehydration during this test. KF analysis was used to measure the water content in the solids at each sample point. Figure 8 shows this dehydration profile in the rotary dryer for the 14 h stress test. As can be seen in Figure 8, the dehydration occurs at a constant rate. This linear profile is consistent with the TGA data, and extrapolation of the profile predicts complete dehydration in the factory-scale dryer after ∼275 h. This is substantially longer than the predicted time of 62 h as observed during the TGA experiments. A hypothesis for the slower dehydration rate in the factory-scale dryer could be due to the significantly smaller sweep rate. Based on the calculated leak rate of ∼1.7 mol/min, the effective sweep rate in the dryer is ∼100 $\mathrm{mL \cdot g^{-1} \cdot min^{-1}}$, about an order of magnitude less than the TGA experiments. This lower sweep rate may have resulted in slower mass transfer of water from the crystal surface to the carrier gas, a limitation that did not exist in the TGA setup. Therefore, due to the variability in the leak rate of a factory-scale dryer, the time for complete dehydration at 40 °C will also be variable.

Since the monohydrate was observed to dehydrate at the stress test conditions in the factory-scale rotary dryer, an online technique was developed to determine the end-of-drying before dehydration could occur. Since there is difficulty in measuring the properties of the solids in the rotary dryer directly because the equipment is continuously rotating, techniques such as NIR (previously shown to be successful in determining the end-of-drying of a monohydrate in other dryer configurations[4−7]) could not be used in this case. Due to the fact that IPA will be preferentially removed from the wetcake before the free water, determining when the free water had been completely removed from the wetcake would be adequate to determine the end-of-drying. This was accomplished by measuring the dew point of the dryer vapor effluent using a dew-point hygrometer that was resistant to the presence of IPA, as shown in Figure 1.

Table 1. **Initial properties of four batches of monohydrate wetcake dried in the rotary dryer step**

batch number	wetcake weight (kg)	IPA content (wt %)	water content (wt %)	total LOD (wt %)	IPA/water ratio of residual solvent (kg/kg)
batch 1A	31.2	2.9	4.3	3.7	78/22
batch 1B	38.6	2.8	4.1	3.4	82/18
batch 1C	27.8	5.0	4.7	6.2	81/19
batch 1D	33.6	8.1	5.4	10.0	81/19

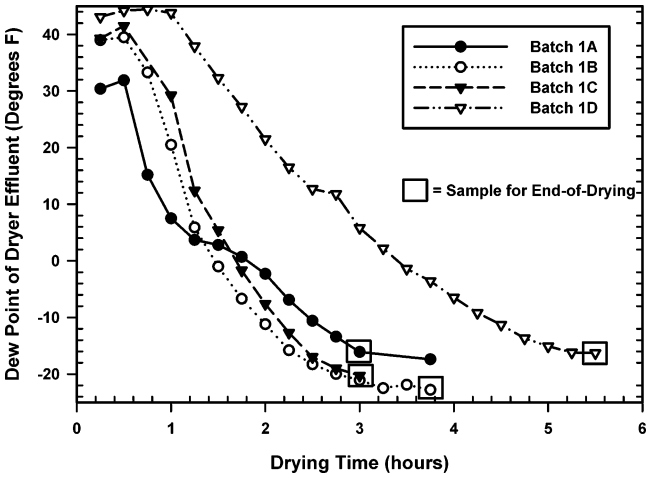

Figure 9. **Dew-point profiles for the dryer vapor effluent for all four batches of monohydrate.**

Table 1 summarizes the initial properties of the four monohydrate wetcake batches dried using this technique. The total loss-on-drying (LOD) of the batches was calculated by adding the water and IPA weight percentages, and subtracting 3.46 wt % due to crystal-bound water that is not free solvent. As can be seen in Table 1, the ratio of IPA/water in the residual solvent in each wetcake batch is nearly identical to the 80/20 (w/w) IPA/water final wetcake wash in the centrifuge, showing consistency between the analytical assays and expected results.

Each batch was dried separately using the rotary dryer/dew-point hygrometer setup discussed earlier. Figure 9 shows the dew-point profile over the course of drying for each batch. A sample for end-of-drying analysis was taken once the dew point became steady, and this sampling point is denoted by a box for each batch in Figure 9. As can be seen in this figure, Batch 1D took longer to reach a steady dew point, consistent with the expectation that this batch would take longer to dry since its initial LOD was significantly greater than any other batch. Also, the final steady dew points

(11) Felder, R.; Rousseau, R. *Elementary Principles of Chemical Processes*; 2nd ed.; John Wiley & Sons: New York, 1986; pp 625−627.
(12) Perry, J. *Chemical Engineers' Handbook*, 3rd ed.; McGraw-Hill: New York, 1950; pp 760−765.

Table 2. **Analytical results for sample pulled from rotary dryer for each batch to determine the end-of-drying**

batch number	sample time (h)	IPA content (wt %)	water content (wt %)	XRD crystal form confirmation
batch 1A	3.0	<0.01	3.50	100% monohydrate
batch 1B	3.75	<0.01	3.47	100% monohydrate
batch 1C	3.0	<0.01	3.51	100% monohydrate
batch 1D	5.5	<0.01	3.50	100% monohydrate

for each batch varied slightly (from −15 to −24 °F). This variation is attributed to varying room humidities and absolute dryer pressures between each batch, which will affect the final dryer relative humidity according to eq 1.

Table 2 presents the results of the sample taken from each batch to call the end-of-drying. For each batch, monitoring the dew point was successful in establishing the end-of-drying without any dehydration of the monohydrate occurring. Also, IPA content in the drycake was not detectable by GC (i.e. <0.01 wt %), consistent with the VLE data simulation presented earlier, and therefore the IPA solvate was never the more favored polymorph during drying.

Although tracking the dew-point profile is sufficient to call the end-of-drying for the monohydrate, these data can also be used to produce a complete drying curve. This is beneficial for informational purposes and could possibly be used to optimize the drying-time cycle. This analysis works only if the dew-point hygrometer is unaffected by the presence of organic vapors, as is the case here.

First, the dew point is converted to a partial pressure of water using dew-point/frost-point tables.[11−12] The mole fraction of water in the vapor is calculated by dividing the partial pressure of water by the total pressure in the dryer effluent line (∼50 Torr for these batches). The mole fraction of water in the dryer effluent line is related to the rate of water removal by eq 2.

$$W_{mf} = \frac{N_{H_2O}}{N_{air} + N_{H_2O} + N_{IPA}} \tag{2}$$

Since the rate at which IPA is removed from the cake is a function of the free solvent composition of the cake (given by the VLE data), eq 2 can be rewritten as eq 3. The mole fraction of IPA in the vapor, y_{IPA}, is a function of the remaining water content of residual solvent on the cake and therefore changes over the course of drying.

$$W_{mf} = \frac{N_{H_2O}}{N_{air} + N_{H_2O} + \left[N_{H_2O}\left(\frac{y_{IPA}}{1 - y_{IPA}}\right)\right]} \tag{3}$$

Equation 3 is solved for N_{H_2O}, or the rate in which water is removed from the dryer, and is given as eq 4.

$$N_{H_2O} = \frac{(W_{mf}) \times N_{air}}{1 - (W_{mf}) - \left[\frac{(W_{mf}) \times y_{IPA}}{1 - y_{IPA}}\right]} \tag{4}$$

In eq 4, W_{mf} is known for a given time interval based on the dew-point measurement of the dryer effluent, N_{air} is simply equal to the estimated leak rate into the dryer (1.7 mol/min), and y_{IPA} is calculated for each time interval using VLE data from an ASPEN simulation (see Figure 4). Since the dew point was recorded every 15 min, the analysis is performed on the basis of the assumption that the measured dew point was constant for the 15 min prior to the measurement. Using an iterative approach to determine the total water removed after n intervals, eq 5 is obtained.

$$L_{H_2O,n} = L_{H_2O,n-1} + [N_{H_2O} \times (\Delta t)] \tag{5}$$

Using eqs 4 and 5 simultaneously in an iterative calculation, the drying curves for all four batches are shown in Figure 10 as the percent of the initial amount of water removed after a specified amount of drying time.

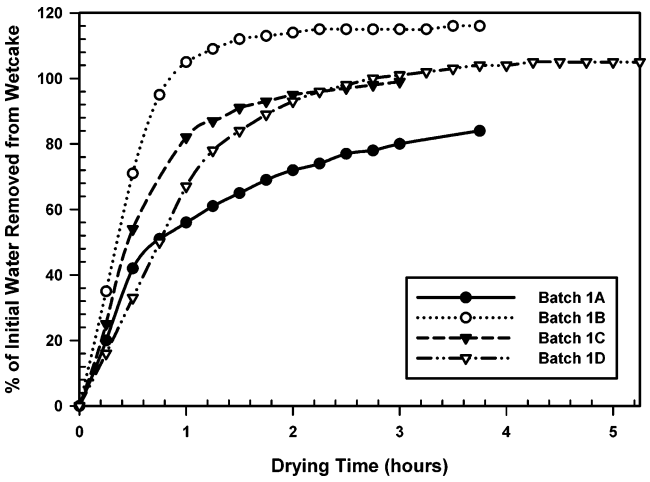

Figure 10. **Drying curves produced using dew-point profile and an iterative calculation approach.**

The drying curves shown in Figure 10 result in overall water removal that varies from 80 to 120% of the initial water content, even though analytical analysis revealed complete removal of free water for all four batches. This discrepancy is due to varying leak rates into the dryer. One of the major limitations of the analysis is the assumption of a constant leak rate, which is known to vary between batches. Also, this analysis neglected ambient water vapor that entered the dryer due to the air leak, which is a good assumption since the water vapor entering the dryer due to the leak is far less than the initial residual water solvent on the wetcake.

Conclusions

A detailed analysis of polymorphic relationships between a desired monohydrate and undesired dehydrated and IPA-solvated species led to a drying procedure that used a dew-point hygrometer to successfully determine the end-of-drying for the monohydrate. Due to the fact that there was a binary residual solvent on the wetcake composed of IPA and water, a dew-point hygrometer was chosen that was unaffected by the presence of IPA vapor. This system allows for an optimized time cycle, ensures that a deliverable product will be generated with each batch, and can be used in any drying process in which water is the final component to be removed from a wetcake. The dew-point hygrometer used to monitor

the dryer vapor effluent presents a new method for online analysis of a factory-scale drying process.

NOMENCLATURE

RH_{dryer} = relative humidity in the dryer (%)
$P^{sat}_{T=40C}$ = saturation pressure of water at 40 °C (Torr)
$P^{atm}_{H_2O}$ = partial pressure of water in the atmosphere at ambient conditions (Torr)
P_{dryer} = absolute pressure in the dryer (Torr)
P_{atm} = atmospheric pressure (Torr)
W_{mf} = mole fraction of water in the dryer vapor effluent (unitless)
N_{H_2O}, N_{IPA}, N_{air} = molar flow rate of water, IPA, and air in the dryer vapor effluent, respectively (mol/min)
y_{IPA} = mole fraction of IPA, neglecting air, in the dryer vapor effluent (unitless)
$L_{H_2O,n}$ = total amount of water removed from dryer after n dew-point time intervals (moles)
Δt = time step between dew-point measurements (min)

Acknowledgment

We thank Joseph Kukura, Elizabeth Fisher, Angela Spartalis, and Russell Ferlita of Merck and Company for their assistance in experimental setups for the drying experiments and characterization of the dry compound.

Received for review February 23, 2004.

OP049956A